SCIENTIFIC REPORTS

OPEN

SUBJECT AREAS:
APPLIED PHYSICS
ELECTRICAL AND ELECTRONIC ENGINEERING
HIGH-ENERGY ASTROPHYSICS
FLUID DYNAMICS

Received
21 August 2012

Accepted
27 December 2012

Published
30 January 2013

Correspondence and requests for materials should be addressed to S.F. (sfujioka@ile.osaka-u.ac.jp)

Kilotesla Magnetic Field due to a Capacitor-Coil Target Driven by High Power Laser

Shinsuke Fujioka[1], Zhe Zhang[1], Kazuhiro Ishihara[1], Keisuke Shigemori[1], Youichiro Hironaka[1], Tomoyuki Johzaki[2], Atsushi Sunahara[3], Naoji Yamamoto[4], Hideki Nakashima[4], Tsuguhiro Watanabe[5], Hiroyuki Shiraga[1], Hiroaki Nishimura[1] & Hiroshi Azechi[1]

[1]Institute of Laser Engineering, Osaka University, 2-6 Yamada-oka, Suita, Osaka 565-0871, Japan, [2]Graduate School of Engineering, Hiroshima University, 1-4-1 Kagamiyama, Higashi-Hiroshima, Hiroshima 739-8527, Japan, [3]Institute for Laser Technology, 2-6 Yamada-oka, Suita, Osaka 565-0871, Japan, [4]Department of Advanced Energy Engineering Science, Kyushu University, 6-1 Kasuga-Koen, Kasuga, Fukuoka 816-8580, Japan, [5]National Institute of Fusion Science, Toki, Gifu 509-5292, Japan.

Laboratory generation of strong magnetic fields opens new frontiers in plasma and beam physics, astro- and solar-physics, materials science, and atomic and molecular physics. Although kilotesla magnetic fields have already been produced by magnetic flux compression using an imploding metal tube or plasma shell, accessibility at multiple points and better controlled shapes of the field are desirable. Here we have generated kilotesla magnetic fields using a capacitor-coil target, in which two nickel disks are connected by a U-turn coil. A magnetic flux density of 1.5 kT was measured using the Faraday effect 650 μm away from the coil, when the capacitor was driven by two beams from the GEKKO-XII laser (at 1 kJ (total), 1.3 ns, 0.53 or 1 μm, and 5×10^{16} W/cm^2).

Laboratory generation of strong, shaped magnetic fields offers a new experimental test bed to study plasma and beam physics[1], astro-[2] and solar-physics[3,4], materials science[5], and atomic and molecular physics[6]. In fast-ignition laser fusion research, collimation of a relativistic electron beam by an axial magnetic field is a key scheme to increase the coupling efficiency between the laser and the core[7]. Magnetic field reconnection[3,4] and collisionless shock generation[1] in a plasma subject to a strong magnetic field are also current research objectives.

Magnetic field is generated spontaneously in a laser-produced plasma[8], and several kilotesla field[9,10] has been measured in a relativistically intense laser-plasma interaction experiment in small spatial and temporal scales. Kilotesla fields have been produced by magnetic flux compression using imploding metal tubes[11] and plasma shells[12–15]. Up to 4 kT has been generated by compressing a 6-T seed magnetic field at the OMEGA laser facility. This magnetic field was used in a central-ignition inertial fusion experiment[13]. The temperature of the hot spot increases by embedding the magnetic field seed in the fusion fuel because the strong field inhibits electron heat conduction to the surrounding cold fuel.

Although the spontaneous magnetic field generation and the flux compression scheme are useful, others techniques are necessary because multipoint accessibility and controlled shape of the field are required for several applications. We have demonstrated that kT magnetic flux densities can be produced using a capacitor-coil target[16].

Results

Figure 1 shows photographs of a capacitor-coil target in side and front views. Two nickel disks are connected by a U-turn coil. Kilojoule, nanosecond laser pulses are focused onto the first disk through a hole in the second disk. A plasma is generated at the first disk, and suprathermal hot electrons with temperatures exceeding 10 keV are emitted from the plasma corona[17]. The hot electrons stream down the electron density gradient ahead of the expanding plasma plume and impact the second disk. The second disk acquires a negative charge, and a large electrical potential develops between the disks. That potential difference drives a current in the U-turn coil. A strong magnetic field pulse is generated in the coil. A previous study of this scheme[18] indicated that 100-T magnetic fields could be created. In those experiments, a pick-up coil probe was used to detect the flux density

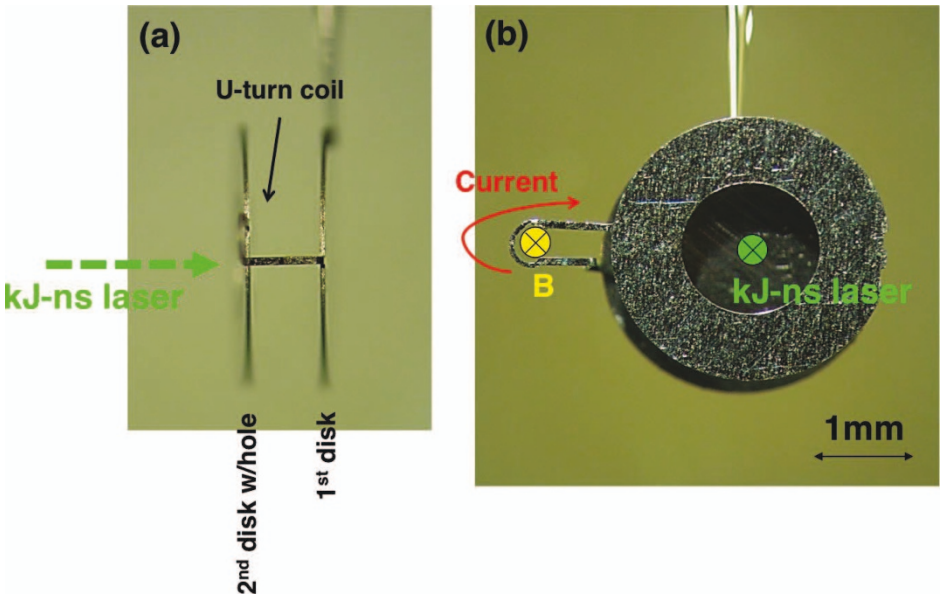

Figure 1 | Photographs of a capacitor-coil target from (a) its side and (b) its front. The two nickel disks are connected by a nickel U-turn coil.

at the coil. However, such probes are susceptible to the electromagnetic noise generated by the laser-plasma interactions.

The Faraday effect is a magneto-optical phenomena, producing a rotation of the plane of polarization that is linearly proportional to the component of the magnetic field in the direction of propagation. The angle of rotation θ is proportional to the length L of the optical path in the medium, the Verdet constant V of the medium, and the magnetic flux density H according to $\theta = L\,V\,H$.

The average value of the flux density within a Faraday medium (B@measure in Table 1) is simply calculated as

$$H_{\text{measure}} = \frac{\theta}{VL}, \tag{1}$$

The thickness (100 or 500 μm) of the Faraday medium is comparable to the distance between the coil and the cylinder. Nonuniformity of the magnetic field in the medium is not negligible. Peak normalized profile of the magnetic flux density along the path of probe, $\hat{H}(x)$ shown in Fig. 2, was calculated with the initial shape of the U-turn coil, where x is a coordinate along the path of probe.

Magnetic flux density at the arbitrary position, $\boldsymbol{H}(x)$, is calculated as

$$H(x) = H_{\text{measure}} \frac{\hat{H}(x)}{\dfrac{\int_{x_F}^{x_R} \hat{H}(x)dx}{x_R - x_F}}, \tag{2}$$

Here x_F and x_R are the positions of the front and rear surfaces of the Faraday medium. In Table 1, magnetic flux densities at 850 μm away from the coil are listed for the comparison.

Figure 3 shows a schematic of the magnetic flux density measurement with Faraday effect[19]. The horizontally polarized second harmonic of a Q-switched Nd:YAG laser (at a wavelength λ of 0.532 μm) was used as the probe light. The probe light pulse is coincident with the GEKKO laser. Fused silica was used as the Faraday medium with a Verdet constant of 298 $\pm$ 12 deg/T m at 0.532 μm. The fused silica has a cylindrical shape whose diameter and length are 600 μm and 100 or 500 μm, respectively. The rear surface is located 600 μm away from the coil, therefore the center of the Faraday medium is 650 or 850 μm away from the coil for the 100 or 500 μm thick medium, respectively.

The transmitted probe light is imaged by lens 1 onto the iris. The central part of the image, having a diameter of 100 μm on the Faraday medium, is selected by the iris. The image is transferred to the visible streak camera by lens 2. Heat absorption and bandpass filters between the iris and lens 2 exclude the laser harmonics and the thermal emission from the plasma. It was experimentally confirmed that the our imaging system detects only the probe light. The Wollaston prism divides the rotated light into horizontal and vertical components.

The equator of the image is selected by a slit on the streak camera cathode in Fig. 3 and the streak image is recorded on a CCD camera. The rotation angle θ is determined from the intensity ratio $I_H/(I_H+I_V) = \cos\theta/(\cos\theta + \sin\theta)$ between the horizontal I_H and vertical I_V components. The temporal resolution is 150 ps.

Figure 4 is a streak image of a magnetic field measurement. A 500 μm-thick cylinder was used as the Faraday medium in this shot (35869). In the reference image, for which a capacitor-coil target was not driven by the GEKKO-XII laser, only the horizontal component was present. When the capacitor-coil target was driven by two beams

Table 1 | Summary of magnetic flux density at 850 μm from the coil

Shot ID	λ_L	E_L	I_L	$I_L\lambda_L^2$	B@measure	B@850 μm	Method
	μm	J	W/cm^2	W/cm^2 μm^2	T	T	
35866	1.053	1000	4.3×10^{16}	4.8×10^{16}	1100 $\pm$ 130	990 $\pm$ 120	FR: 500 μm
35870	1.053	990	2.1×10^{16}	2.3×10^{16}	1500 $\pm$ 330	880 $\pm$ 190	FR: 100 μm
35869	1.053	740	1.6×10^{16}	1.7×10^{16}	480 $\pm$ 60	430 $\pm$ 60	FR: 500 μm
35868	0.526	190	4.1×10^{15}	1.1×10^{15}	180 $\pm$ 50	160 $\pm$ 50	FR: 500 μm
35477	0.526	540	8.2×10^{14}	2.2×10^{14}	N/A	33 $\pm$ 8	Pickup coil

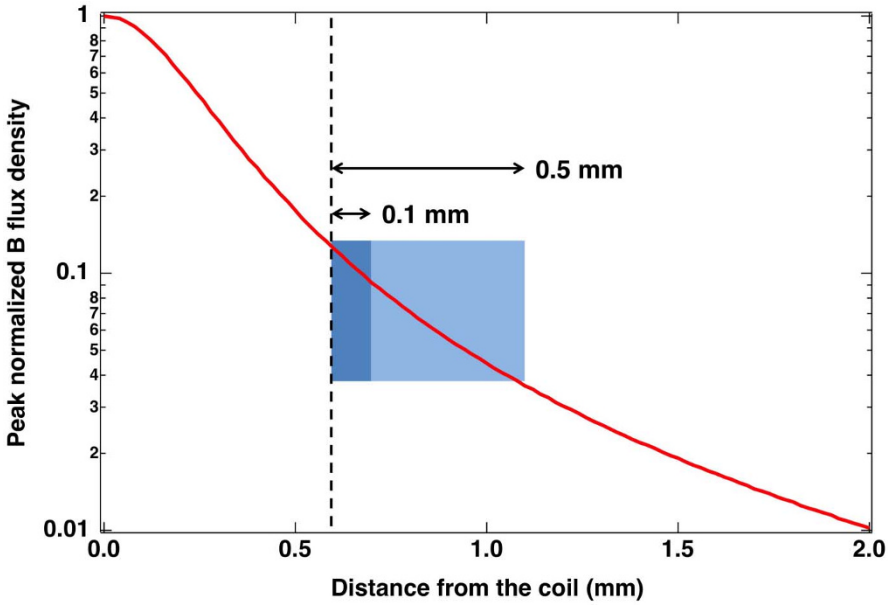

Figure 2 | Peak normalized profile of the magnetic flux density along the path of probe, which was calculated with the initial shape of the U-turn coil used in this experiment. The surface of the Faraday medium was located at 600 μm away from the coil. 100 μm or 500 μm-thick fused silica cylinder was used as the Faraday medium.

of the laser, a vertical component appears and the horizontal component disappears 1.5 ns after the laser irradiation. This delay in the magnetic field indicates that the second disk needs 1.5 ns to acquire hot electrons to drive current in the coil. The intensity ratio was 0.26 $\pm$ 0.07, corresponding to 71 $\pm$ 6 degrees of rotation. The average density of magnetic flux in the Faraday medium is calculated to be 480 $\pm$ 60 T from the rotation angle and a Verdet constant. It was found that the probe light was blocked soon after the magnetic field generation.

Maximum rotation angle of 162 $\pm$ 7 deg. was obtained with a 500 μm-thick fused silica cylinder in the highest intensity shot (35866). The thickness of a cylinder was changed from 500 μm to 100 μm to confirm that the rotation is occurred in the cylinder. Rotation angle of 45 $\pm$ 8 deg. was obtained with a 100 μm-thick cylinder (35870). Positions of the cylinder center (650 μm or 850 μm) were different, two laser beams were not overlapped correctly in the shot (35870), and the intensity was a half of the highest intensity. With the consideration of the above differences, the

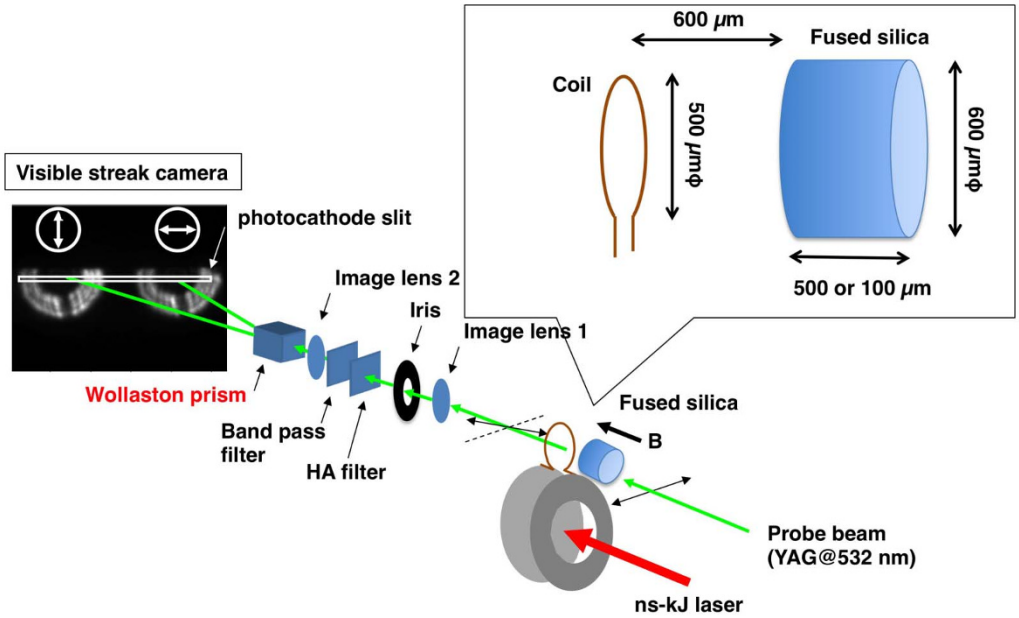

Figure 3 | Magnetic flux density measurement using the Faraday effect. A cylinder made of fused silica, whose diameter and length are respectively 600 μm and 500 or 100 μm, is located away from the coil. Horizontally polarized second-harmonic light from a Nd:YAG laser is used as the probe. The transmitted probe light is imaged by lens 1 onto the iris. The central part of the image, having a diameter of 100 μm on the Faraday medium, is selected by the iris. The image is transferred to the visible streak camera by lens 2. Heat absorption and bandpass filters between the iris and lens 2 exclude the laser harmonics and the thermal emission from the plasma. The Wollaston prism divides the rotated light into horizontal and vertical components.

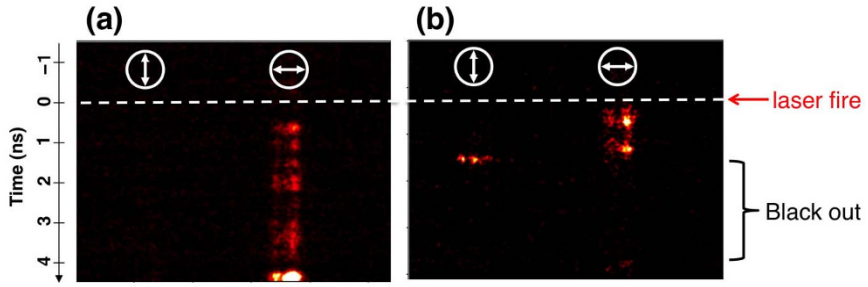

Figure 4 | **Streak images of the horizontal and vertical components of the probe beam in (a) the reference and (b) the magnetic field generation (35869) shots.**

dependence of the rotation angle on the cylinder thickness supports that the rotation is occurred dominantly in the cylinder.

The transmittance of the fused silica recovered within the duration of the probe light pulse in one shot (35870). The temporal evolution of the magnetic flux density was calculated from the intensity ratio. Dynamics of a plasma between the two nickel disks was simultaneously observed from the side using an x-ray imaging system coupled to an x-ray streak camera.

Figure 5(a) plots the evolution of the magnetic flux density measured with the Faraday effect. The hatched region indicates the duration of the probe pulse black out. Figure 5(b) shows an x-ray streak image of the plasma. The zero of time is the beginning of the laser irradiation. The magnetic field develops at 1.5 ns in Fig. 5(a), and a plasma is generated at the second disk at this same time as shown in Fig. 5(b). Consequently, hot electrons with an expansion speed of 5.1×10^7 cm/s arrive at the second disk and produced a plasma. The magnetic field once disappears at 3.0 ns in Fig. 5(a), but plasma emission at the second disk increases at that time. A plasma plume with an expansion speed of 2.5×10^7 cm/s may arrive at 3.0 ns after the laser irradiation. The resulting potential difference drives the current in the plume.

We measured the magnetic flux densities by varying the intensity and wavelength of the drive laser and the thickness of the fused silica cylinder to obtain a scaling law of the flux density against laser intensity and wavelength. Table 1 and Fig. 6 summarize the maximum magnetic field obtained. Average values of magnetic flux density within the Faraday medium (B@measure) and the flux density at 850 μm away from the coil (B@850 μm) were listed in Table 1. The maximum value of the magnetic flux density measured in this experiment was 1500 ± 330 T, 650 μm away from the coil. The dotted line in Fig. 6 shows a liner line as $B(I_L) = 2.7 \times 10^{-14} I_L$. Peak density of the magnetic flux seems to be in proportional to laser intensity not product of intensity and the square of laser wavelength.

A pick-up coil probe was also used to detect the magnetic flux density in the lowest laser intensity shot (35477). The diameter of the pick-up coil was 5 mm and the coil was located at 100 mm from the capacitor-coil target. The pick-up signal is easily affected by electromagnetro noise generated by laser-plasma interactions. In our experimental conditions, we obtained a meaningful signal only at the lowest intensity and a green laser irradiation.

Magnetic field spontaneously generated by laser-plasma interactions overlaps as background on a signal. A planar nickel disk without a coil was irradiated by the laser and the spontaneous field was measured with the pick-up coil. The field density generated with the U-turn coil was ten times higher than the spontaneous one, and direction of the spontaneous field is different from that of the field

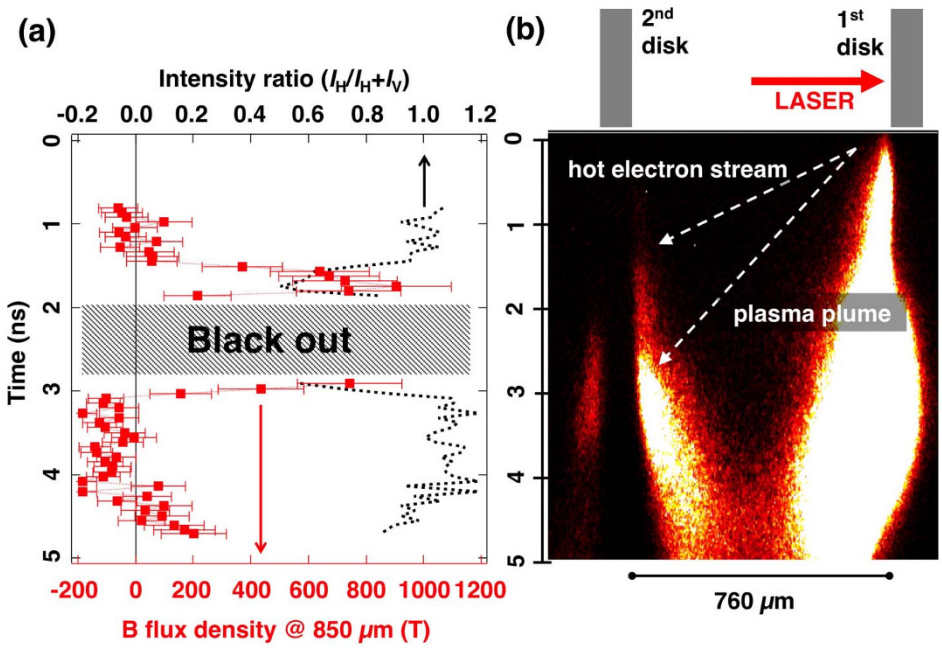

Figure 5 | (a) Temporal evolution of the intensity ratio between horizontal and vertical components and the magnetic flux density using 100-μm-thick fused silica cylinder. The hatch marks in the graph represent the duration of that the probe light was blocked. (b) An x-ray streak image of the plasma generated in the target capacitor.

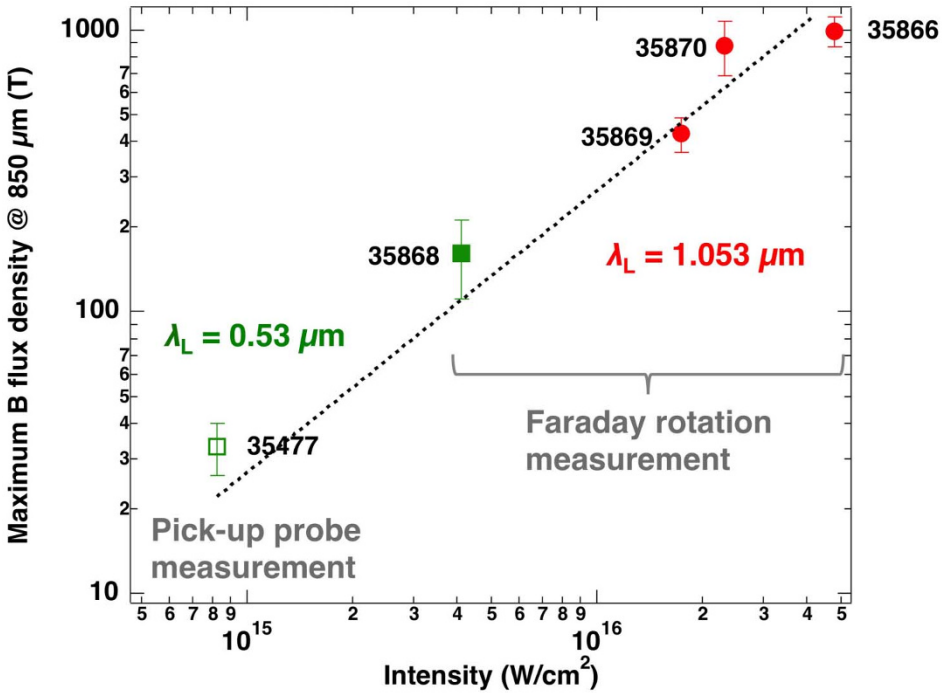

Figure 6 | Variation of the magnetic flux density at 850 μm from the coil as a function of the laser intensity. The red circles and green squares represent the flux density generated by a 1.064-μm laser and a 0.526-μm laser, respectively. The closed or closed marks represent results obtained with the Faraday rotation or the pick-up coil measurements. The dotted line shows a liner line as $B(I_L) = 2.7 \times 10^{-14} I_L$.

generated by the U-turn coil, therefore, we neglected the spontaneous field in the Faraday rotation measurement.

Figure 7 shows temporal change of the magnetic flux density measured with the pick-up coil. The field decays with a characteristic time of 28 ns that is not so far from the decay time of a closed circuit with characteristic $L/R = 17$ ns, where $R \sim 5.4 \times 10^{-2}\,\Omega$ and $L \sim 9.2 \times 10^{-10}$ H were used, respectively. The deep dip around 3 ns is found in the evolution of the field. This phenomenon is found also in the Faraday rotation measurement as shown in Fig. 5, but the mechanism is not clear. Peak flux density was 33 ± 8 T, this is also shown in Fig. 6 and Table 1.

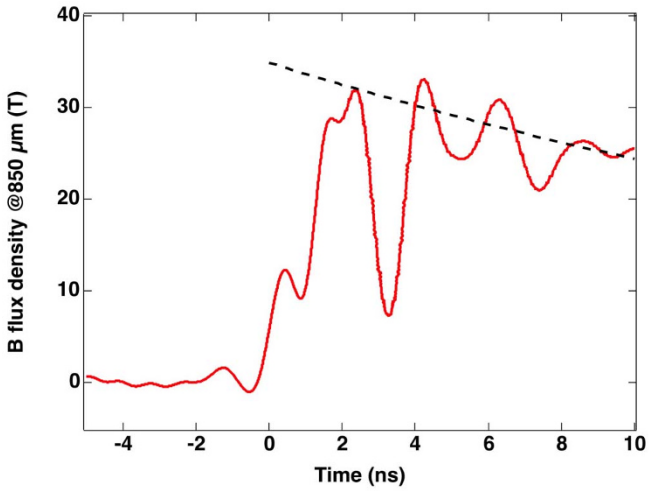

Figure 7 | Temporal evolution of the magnetic field measured with a pick-up coil. The dotted line is an exponential curve with the decay time of 28 ns.

Discussion

The first important discussion issue is a validity of the Faraday rotation measurement for large B and dB/dt achieved in this experiment. In our experiment, B and dB/dt reach 1.5 kT and 3 kT/ns, respectively. Faraday rotation angles for a GaP crystal at a wavelength of 632.8 nm were measured as a function of a field strength up to 400 T measured by a pick-up coil[20]. The rotation angle shows a linear increase with the field strength and the coefficient of 10100 deg/T m that is very close to the value measured at weak field strength (10050 deg/T m).

The Faraday rotation in a fused silica fiber was recently used in magnetic compression experiment with a laser-accelerated foil and a cavity[15]. The time history of the magnetic field during the compression was successfully measured, measured amplification agrees with the ratio between initial and final dimensions of the field embedded area. B and dB/dT reached 800 T and 1 kT/ns in their experiment, therefore this result reveals that the Faraday rotation measurement can be used for at least $B < 800$ T and $dB/dt < 1$ kT/ns.

Validity of the Faraday rotation measurement for the large B and dB/dt achieved in this experiment is still an open question, however, nonlinearity of the Faraday effect induced by large B and dB/dt seems not to cause a significant error in the estimation of field strength, because those two values obtained in our experiment are only two or three times larger than the experimentally validated values.

The second discussion issue is total energy of the magnetic field generated by the laser-driven capacitor coil. By comparing the measured field density and that calculated with the initial shape of the U-turn coil, current in the coil and total energy of the field were estimated to be 8.6 MA and 15 kJ. The field energy was obtained by integrating magnetic field energy (B^2/μ_0) at the field peak timing in the calculation space ($2 \times 4 \times 5$ mm^3). The total energy is inconceivable, because 15 kJ is much larger than the laser energy (1 kJ). Explosion of the coil due to ohmic heating by a large current and consequent implosion of the field inside the coil is a candidate mechanism to explain the experimental result, but we have no experimental evidence for that. Black-out of the probe light found in the

Table 2 | Verdet constant of fused silica at various wavelengths

λ	V
nm	deg T^{-1} m^{-1}
632	212.213[35]
589	274.550[35]
546.1	288.477[36]
435.8	472.837[36]
334.2	859.462[36]
302.2	1099.53[36]
284.8	1271.95[36]

Faraday rotation measurement may be explained by the coil implosion, because the probe light is blocked when the imploding coil collides at the center of the coil. Only a small portion of the magnetic field (100 μm in diameter and 500 μm in length) was measured in the experiment, spatial distribution of the magnetic field must be measured to conclude why the strong field is generated by the laser-driven capacitor-coil target. This measurement is a future work.

One advantage of this scheme is it enables various magnetic field geometries. The GEKKO-XII facility has twelve nanosecond laser beams, and a magnetic mirror or cusp geometry can be produced by using two or four capacitor-coil targets, each driven by two or three laser beams. This geometry affords novel experiments in magnetic field reconnection, as occurs in the solar corona and has previously been studied with a self-generated magnetic field[21–25]. It can also be used to study collisionless shock[26–30] which is a possible mechanism for high-energy particle acceleration and cosmic-ray generation. Dynamics of electron-positron plasmas can be investigated by interactions between an intense laser and a high-Z material in this strong magnetic field[31,32].

Astronomers are interested in the x-ray spectrum of pulsars in the presence of megatesla magnetic fields[2]. Intensity dips[2] are observed in the continuum spectrum. One explanation for these dips is Compton scattering in a Landau-quantized plasma. When the cyclotron radius of an electron in a strong magnetic field is small compared to its de Broglie wavelength and the allowed energy levels are discretized, then absorption bands appear. An energy gap $\Delta E = \hbar\omega_c = \hbar\frac{eB}{m_e}$ equal to 0.1 eV at 1 kT arises in the extreme ultraviolet range.

Methods

Experimental details. Two laser beams at GEKKO-XII were used to drive the capacitor-coil target. The maximum total laser energy, minimum laser spot diameter, pulse duration, and wavelengths were 1000 J, 50 μm, 1.2 ns, and 1.053 or 0.53 μm, respectively.

The capacitor-coil target was designed based on previous work[16,18]. The target consists of two 50-μm-thick nickel disks and a U-turn coil made of 50 μm × 50 μm nickel rod. The diameter of the disk is 3568 μm and the diameter of the hole in the first disk is 1784 μm, to prevent the GEKKO beams from hitting the periphery of the hole. The separation between the two disks is 780 μm, limited by the fraction of the hot electrons that do not reach the second disk due to the $E \times B$ drift in the self-generated magnetic field around the plasma. The radius of curvature of the U-turn coil is 500 μm. A glass stalk, used to support the target in the vacuum chamber, is connected to the first disk.

The probe laser had multiple peaks in time-domain due to multi-mode operation of a laser oscillator without a single-mode seeding light, envelope of the probe pulse had 7 ns of full width at half maximum. The probe beams was shaped with a 1-mm-diameter aperture, the shaped probe beam passed through the Faraday medium. Energy of the probe beam was adjusted by inserting several filters in the laser path to the acceptable energy for a visible streak camera.

Verdet constant at 532 nm. The Verdet constant depends on the wavelength of the probe. It was calculated for 532 nm light by a model. The Verdet constant V (in rad T^{-1} m^{-1}) depends on the wavelength (in nm) according to[33]

$$V(\lambda) = \frac{e}{2mc^2}\gamma\lambda\frac{dn(\lambda)}{d\lambda} \tag{3}$$

where e, m, and c are the electron charge, electron mass, and speed of light. Here γ is the magnetooptical anomaly equal to 0.692. The dispersion in the refractive index is[34]

$$n^2(\lambda) = 1 + \frac{0.6961663\lambda^2}{\lambda^2-(0.0684043)^2} + \frac{0.4079426\lambda^2}{\lambda^2-(0.1162414)^2} + \frac{0.8974794\lambda^2}{\lambda^2-(9.896161)^2}. \tag{4}$$

Consequently the Verdet constant at 532 nm is calculated to be 287 deg/T m.

By another method, the Verdet constant at 532 nm was determined to be 310 deg/T m by interpolation of data[35,36] listed in Table 2. fitted to the power law

$$V(\lambda) = \frac{4.13539\times10^8}{\lambda^{2.2455}}. \tag{5}$$

$V = 298 \pm 12$ deg/T m is used in the this study as a Verdet constant of a fused silica at 0.532 μm.

Error in estimation of magnetic flux density from faraday rotation. Intensity ratio between horizontal and vertical components of the rotated light ($I_H/(I_H + I_V)$) has fluctuation of $\pm$ 0.07 of a typical value. This fluctuation was considered in the calculation of the rotation angle from the intensity ratio. Uncertainly of Verdet constant of a fused silica at 0.532 μm light ($V = 298 \pm 12$ deg./T m) was considered in the calculation of the magnetic flux density from the rotation angle. The upper and lower values of the flux density were calculated by using $V = 286$ and 310 deg./T m from the rotation angle, respectively. Consequent error was in the range from $\pm$ 12 to $\pm$ 31% of the flux density.

1. Sagdeev, R. Z. *Reviews of Plasma Physics, chap.* Cooperative Phenomena and Shock Waves in Collisionless Plasmas, 23 (Consultants Bureau, New York, 1966).
2. Santangelo, A. *et al.* A BEPPOSAX study of the pulsating transient X0115+63: The first X-ray spectrum with four cyclotron harmonic features. *Astro. Phys. J. Lett.* **523**, L85 (1999).
3. Kopp, R. A. & Pneuman, G. W. Magnetic reconnection in the corona and the loop prominence phenomenon. *Solar Phys.* **50**, 85 (1976).
4. Masuda, S., Kosugi, T., Hara, H., Tsuneta, S. & Ogawara, Y. A loop-top hard x-ray source in a compact solar flare as evidence for magnetic reconection. *Nature* **371**, 495 (1994).
5. Herlach, F. & Miura, N. (eds.) *High Magnetic Fields: Science and Technology* (World Scientific Pub Co Inc, Singapore, 2003).
6. Gilch, P., Pöllinger-Dammer, F., Musewald, C., Michel-Beyerle, M. E. & Steiner, U. E. Magnetic field effect on picosecond electron transfer. *Science* **281**, 982 (1998).
7. Strozzi, D. J. *et al.* Fast-ignition design transport studies: Realistic electron source, integrated PIC-hydrodynamics, imposed magnetic fields. *Phys. Plasma* **19**, 072711 (2012).
8. Stamper, J. A., Papadopoulos, K., Sudan, R. N., Dean, S. O. & McLean, E. A. Spontaneous magnetic fields in laser-produced plasmas. *Phys. Rev. Lett.* **26**, 1012 (1971).
9. Tatarakis, M. *et al.* Measuring huge magnetic field. *Nature* **415**, 280 (2002).
10. Wagner, U. *et al.* Laboratory measurements of 0.7 GG magnetic fields generated during high-intensity laser interactions with dense plasmas. *Phys. Rev. E* **70**, 026401 (2004).
11. Takeyama, S., Sawabe, H. & Kojima, E. Recent developments of the electromagnetic flux compression. *J. Low Temp. Phys.* **159**, 328 (2010).
12. Knauer, J. P. *et al.* Compressing magnetic fields with high energy lasers. *Phys. Plasmas* **17**, 056318 (2010).
13. Chang, P. Y. *et al.* Fusion yield enhancement in magnetized laser-driven implosions. *Phys. Rev. Lett.* **107**, 035006 (2011).
14. Hohenberger, M. *et al.* Inertial confinement fusion implosions with imposed magnetic field compression using the OMEGA laser. *Phys. Plasmas* **19**, 056306 (2012).
15. Yoneda, H. *et al.* Strong compression of a magnetic field with a laser-accelerated foil. *Phys. Rev. Lett.* **109**, 125004 (2012).
16. Daido, H. *et al.* Generation of a strong magnetic field by an intense co2 laser pulse. *Phys. Rev. Lett.* **56**, 846 (1986).
17. Forslund, D. W., Kindel, J. M. & Lee, K. Theory of hot-electron spectra at high laser intesity. *Phys. Rev. Lett.* **39**, 284 (1977).
18. Courtois, C., Ash, A. D., Chambers, D. M., Grundy, R. A. D. & Woolsey, N. C. Creation of a uniform high magnetic-field strength environment for laser-driven experiments. *J. Appl. Phys.* **98**, 054913 (2005).
19. Hasegawa, N. *et al.* High-resolution spectroscopy of the nickel-like molybdenum X-ray laser toward the generation of circularly polarized X-ray laser. *Journal of Optical Society of Korea* **13**, 60 (2009).
20. Miura, N. Solid state physics in megagauss fields generated by electromagnetic flux compression and single-turn coils. *Phys. B.* **201**, 40 (1994).
21. Yates, M. A., van Hulsteyn, D. B., Rutkowski, H., Kyrala, G. & Brackbill, J. U. Experimental evidence for self-generated magnetic fields and remote energy deposition in laser-irradiated targets. *Phys. Rev. Lett.* **49**, 1702 (1982).
22. Nilson, P. M. *et al.* Magnetic reconnection and plasma dynamics in two-beam laser-solid interactions. *Phys. Rev. Lett.* **97**, 255001 (2006).
23. Li, C. K. *et al.* Observation of megagauss-field topology changes due to magnetic reconnection in laser-produced plasmas. *Phys. Rev. Lett.* **99**, 055001 (2007).
24. Nilson, P. M. *et al.* Bidirectional jet formation during driven magnetic reconnection in twobeam laser–plasma interactions. *Phys. Plasma* **15**, 092701 (2008).

25. Zhong, J. *et al.* Modelling loop-top X-ray source and reconnection outflows in solar flares with intense lasers. *Nat. Phys.* **6**, 984 (2010).
26. Taylor, R. J., Baker, D. R. & Ikezi, H. Observation of collisionless electrostatic shocks. *Phys. Rev. Lett.* **24**, 206 (1970).
27. Ikezi, H., Kamimura, T., Kako, M. & Lonngren, K. E. Laminar electrostatic shock waves generated by an ion beam. *Phys. Fluids* **16**, 2167 (1973).
28. Courtois, C. *et al.* Experiment on collisionless plasma interaction with applications to supernova remnant physics. *Phys. Plasmas* **11**, 3386 (2004).
29. Bailung, H., Nakamura, Y. & Saitou, Y. Observation of ion-acoustic shock wave transition due to enhanced Landau damping. *Phys. Plasmas* **15**, 052311 (2008).
30. Kuramitsu, Y. *et al.* Time evolution of collisionless shock in counterstreaming laser-produced plasmas. *Phys. Rev. Lett.* **106**, 175002 (2011).
31. Cowan, T. E. *et al.* High energy electrons, nuclear phenomena and heating in petawatt lasersolid experiments. *Laser Part. Beam* **17**, 773 (1999).
32. Wilks, S. C. *et al.* Electron-positron plasmas created by ultra-intense laser pulses interacting with solid targets. *Astro. Space Sci.* **298**, 347 (2005).
33. Munin, E., Roversi, J. A. & Villaverde, A. B. Faraday-effect and energy-gap in opticalmaterials. *J. Phys. D* **25**, 1635 (1992).
34. Kitamura, R., Pilon, L. & Jonasz, M. Optical constants of silica glass from extreme ultraviolet to far infrared at near room temperature. *Appl. Optics* **46**, 8118 (2007).
35. Mitscheke, F. *Fiber Optics: Physics and Technology* (Springer, 2009).
36. Kaye, G. W. C. & Laby, T. H. (eds.). *Tables of Physical and Chemical Constants and Some Mathematical Functions (16th edition)* 143 (Longmans, London, 1995).

Acknowledgements

The authors thank the technical support staff at the GEKKO-XII facility for laser operation, target fabrication, and plasma diagnostics. The authors acknowledge Dr. N. Hasegawa (JAEA) and Dr. K. Kondo (TIT) for valuable contributions to this experiment. The authors also thank Prof. J. Honrubia (UPM), Prof. F. Wang (NAO at CAS), Dr. T. Enoto (RIKEN), Dr. D. Salzmann (WI), and Prof. H. Takabe (ILE) for fruitful discussions. This research was supported by the Japanese Ministry of Education, Science, Sports, and Culture (MEXT), by Special Education and Research Expenses for 'Laboratory Astrophysics with High-Power Laser' and a Grant-in-Aid for Young Scientists (A) for 'Extreme Magnetic Field Generation for Quantum Beam Control and Laboratory X-ray Astronomy (No. 24684044),' Collaboration Research program by NIFS (NIFS12KUGK057 and NIFS11KUGK054) and by the Institute of Laser Engineering at Osaka University (under contract 'Laboratory X-ray Astrophysics with Strong Magnetic Field').

Author contributions

S.F. is the principal investigator who proposed and organized the experiment. Z.Z. and I.K. prepared, conducted, and analyzed the Faraday rotation measurement. K.S. and Y.H. developed the imaging system used in the measurement. This work was motivated by fast-ignition simulations done by T.J. and A.S., while N.Y. and H.N. gave advice on magnetic-field measurements. T.W. carried out the calculation of the magnetic field structure. H.N. is a coordinator of this experiment, and H.S. and H.A. are the leaders of the project.

Additional information

Competing financial interests: The authors declare no competing financial interests.

License: This work is licensed under a Creative Commons Attribution-NonCommercial-NoDerivs 3.0 Unported License. To view a copy of this license, visit http://creativecommons.org/licenses/by-nc-nd/3.0/

How to cite this article: Fujioka, S. *et al.* Kilotesla Magnetic Field due to a Capacitor-Coil Target Driven by High Power Laser. *Sci. Rep.* **3**, 1170; DOI:10.1038/srep01170 (2013).